

## EFFECT OF ROTOR'S ANGULAR SPEED AND ASPECT RATIO ON ENTROPY GENERATION IN A ROTOR-CASING ASSEMBLY

Bassam ABU-HIJLEH, Jiyuan TU, and Aleksandar SUBIC

School of Aerospace, Mechanical & Manufacturing Engineering, RMIT University  
 PO Box 71 Bundoora, Vic 3083 - AUSTRALIA

### ABSTRACT

CFD is used to simulate the flow field in a rotor-casing assembly. The simulation was carried out for different elliptic rotor aspect ratios (AR), inlet flow velocities, and rotor angular speeds. The flow field results were used to ascertain the changes in quantities that affect the efficiency of a rotor-casing assembly. This included changes in traditional quantities such as: inlet pressure, magnitude of the maximum velocity, and maximum turbulence. Integrated entropy generation was also calculated. Of the different traditional quantities reported, the inlet pressure results were closest to the entropy generation results. Overall, the results indicate that a rotor's  $AR > 2$  increases the efficiency of a rotor-casing assembly, which becomes almost constant for  $AR > 5$ .

### NOMENCLATURE

$AR$	rotor aspect ratio ( $a/b$ )
$a$	rotor major radius
$b$	rotor minor radius
$CL$	rotor-casing clearance ( $[(10-a)/10]*100\%$ )
$KE_{max}$	maximum turbulent kinetic energy
$k$	thermal conductivity
$P$	pressure
$S''$	rate of entropy generation per unit area
$S_{tot}$	total entropy generation
$T$	temperature
$V_{in}$	inlet velocity
$V_{max}$	maximum velocity
$\omega$	angular speed ratio ( $\omega * a / V_{in}$ )
$\mu$	dynamic viscosity
$\omega$	rotor angular speed

### INTRODUCTION

Engine power rating represents an important selling point in the automotive industry. The need for more engine power in the automotive industry has traditionally been fulfilled by using bigger engines. During the majority of actual driving conditions the engine is required to generate a small fraction of its rated peak power. The use of big engines to develop the small power needed for day-to-day motoring conditions is an expensive and inefficient practice. The high level of air pollutants produced by the automobile engines has further exasperated this issue (Takei and Takabe, 1997). The pollutant production is, among other factors, proportional to the size of the engine and its operating conditions. Thus the automotive industry requires a small engine that can deliver the peaking high power performance of large engines yet still be economical and environmentally friendly at the nominal

operating conditions of day-to-day driving. The answer to this issue has been the addition of different types of power-boosting devices to small engines. This is achieved by forcing denser air into the engine's cylinders. Increasing the air density is achieved primarily by compressing the atmospheric air before it is fed into the engine's cylinders. This can be achieved in many ways but the most common methods are turbocharging and supercharging (Heisler, 2001).

The effect of the rotor's aspect ratio on the energy losses in a rotor-casing assembly, used as a model of a power-boosting device, is addressed numerically in this paper. This work is part of a major, multi-disciplinary, supercharger research program at the Department of Mechanical Engineering – RMIT. The new designs will be used in conjunction with current and future supercharger prototypes under investigation. FLUENT, a commercial Computational Fluid Dynamics (CFD) package is used to simulate the flow field. The turbulent flow is solved using the Renormalised Group Theory (RNG) turbulence model over a Finite Volume (FV) grid. A User Defined Function (UDF) was coupled with FLUENT and used to calculate the local and the integrated total entropy generation in the flow field based on the detailed velocity field calculations.

### MODEL DESCRIPTION

Figure (1) shows a schematic of the flow field under consideration. All length scales in figure (1) are in centimetres but the schematic is not to scale. The casing radius was fixed at 10 cm. The rotor cross-section is an ellipse. The rotor-casing clearance (CL) was varied by changing the rotor's major radius ( $a = 8$  and  $9.8$  cm). This translated to a CL of 20% and 2%, based on the casing radius. The parameters studied in this paper included: rotor aspect ratio ( $AR \equiv a/b = 1, 1.25, 2, 5, 10$ ), inlet velocity ( $V_{in} = 1, 5, 10$  m/s), angular speed ratio ( $\omega = 0.1, 1, 10$ ), and rotor-casing clearance ( $CL = 2\% \& 20\%$ ).

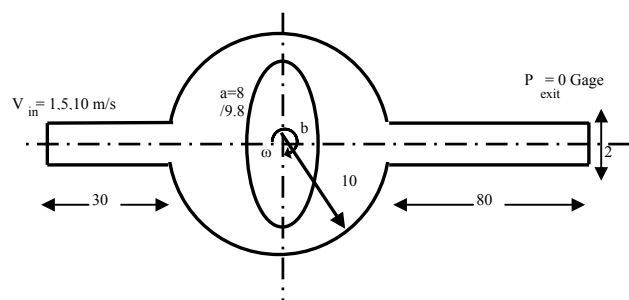


Figure 1: Schematic of the rotor-casing assembly including relevant dimensions (in cm).

The angular speed ratio is intended to look at the changes in the effect of the rotor's aspect ratio as a function of its contribution to the total velocity inside the casing. At AR=1, the ellipse is a circle. This value is used to show the lower limit of AR.

FLUENT solves the Reynolds-Averaged Navier-Stokes (RANS) equations over a finite volume grid. Second order upwind discretisation was used for the momentum and turbulence equations. Second order implicit time formulation was also used. A sliding mesh was used around the rotor and a stationary mesh for the rest of the assembly. The RNG modified K- $\epsilon$  turbulence model was used to model the turbulence quantities that arise from the time averaging process. At high Reynolds number, RNG is similar to the standard K- $\epsilon$ , but RNG has special treatment for the effective viscosity at low Reynolds number (Mohammadi and Pironnean, 1993). This is particularly important in flows where there are flow separation, reattachment, and recirculation zones (Abu-Hijleh, 2000). In modelling the outlet as a pressure-outflow boundary condition, the location of the outlet was placed far enough not to affect the flow field in the casing. Other modelling checks included mesh independence, residual convergence value, and time step. For example, quadrupling the number of cells from 13200 to 52800 resulted in less than a 2% change in the values being monitored in this study. Based on these tests, a fixed mesh size of 13200 cells was used for all configurations; Fig. (2). The residual convergence value used was 1E-4. The solution was advanced in (w) dependent time steps equivalent to a 1-degree rotation of the rotor. This value was chosen based on several tests to determine the solution stability at different time increments. Due to the symmetry of the rotor and the casing, the unsteady simulation covered only 180 degrees. The "velocity inlet" boundary condition was used at the inlet with a 1% turbulence intensity (Fluent, 2002). The "pressure outlet" boundary condition was used at the exit (Fluent, 2002).

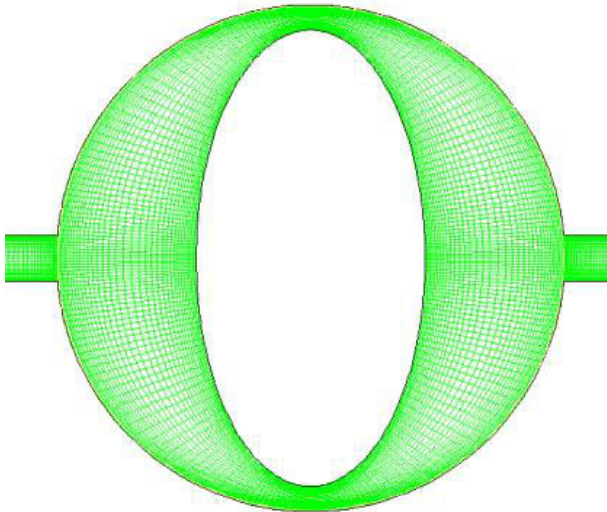


Figure 2: Close-up of the grid used.

Entropy calculation was used to assess the thermodynamic efficiency of the different inlet/outlet fillet configurations. Entropy is a fundamental property based on the second law of thermodynamics and can account for all types of irreversibility in a system. The 2D local entropy generation equation can be written as (Bejan, 1982):

$$\dot{S} = \frac{k}{T^2} \left[ \left( \frac{\partial T}{\partial x} \right)^2 + \left( \frac{\partial T}{\partial y} \right)^2 \right] + \frac{\mu}{T} \left[ 2 \left( \frac{\partial u}{\partial x} \right)^2 + 2 \left( \frac{\partial v}{\partial y} \right)^2 + \left( \frac{\partial u}{\partial y} + \frac{\partial v}{\partial x} \right)^2 \right] \quad (1)$$

Where  $\dot{S}$  is the rate of entropy generation per unit area, for a 2D case. The first term of the RHS represents entropy generation due to thermal effects while the second term represents entropy generation due to viscous effects. Thermal effects were not considered in this study and thus only the second term was calculated. The total entropy generation was calculated by integrating the local values over the entire flow field domain between the inlet and outlet.

## RESULTS

The effect of rotor aspect ratio on the overall flow field was studied by focusing on the changes in the pressure difference between inlet & outlet, maximum velocity, maximum turbulence levels, and total entropy generation. All results were integrated and time averaged over  $\frac{1}{2}$  a cycle (180 degrees) due to symmetry. The results were subsequently partially normalised by the proper factor of the inlet velocity, e.g. inlet static pressure ( $P_{in}$ ) was normalised by  $V_{in}^2$  only without using  $0.5 \rho$ . The maximum velocity ( $V_{max}$ ), maximum turbulence ( $KE_{max}$ ), and total entropy generation ( $S_{tot}$ ) were normalised using  $V_{in}$ ,  $V_{in}^2$ , and  $V_{in}^3$ , respectively.

Figure 4 shows the changes in the normalized  $P_{in}$ ,  $V_{max}$ ,  $KE_{max}$ , and  $S_{tot}$  as a function of the rotor aspect ratio for the case of CL=2%. This figure shows that the use of high aspect ratio rotors, AR>2, results in higher thermodynamic efficiency. Increasing the rotor's AR beyond 5 resulted in little change in the efficiency. It can be seen that only the  $P_{in}$  trend is compatible with that of  $S_{tot}$ . At times,  $V_{max}$  and  $KE_{max}$  give contradicting results to those of  $P_{in}$ ,  $S_{tot}$ , and even each other. The problem with these two traditional quantities is that they focus on a localized segment of the flow field without due consideration of the remainder of the flow field. For example,  $KE_{max}$  gives an indication of the maximum turbulence at some point within the flow field but without consideration of the turbulence intensity distribution in the remainder of the flow field. A high level of localized turbulence ( $KE_{max}$ ) coupled with low turbulence levels in the remainder of the flow field is less problematic than a somewhat lower  $KE_{max}$  that is almost uniform across the flow field. Figure 3 shows the changes in the normalized  $P_{in}$ ,  $V_{max}$ ,  $KE_{max}$ , and  $S_{tot}$  as a function of the rotor aspect ratio for the case of CL=20%. The general trend is similar to that in figure (2), the main feature being the lower levels of pressure, turbulence, and entropy. The wider clearance results in significantly lower pressure requirements and losses.

This is a clear indication of the need for a global and fundamental quantity that can account for all types of losses throughout the flow field. For simple geometries without heat transfer, inlet static pressure can provide such a measure. But in today's complex systems, which integrate several components and include significant thermal effects, static pressure cannot be used to evaluate the efficiency of such systems. Also static pressure does not give any insight as to the locations and/or components that are responsible for high entropy generation rates, i.e. the least efficient. The contours of the local entropy generation can identify regions and/or components responsible for high rates of entropy generation. This is true in all types of flow fields even those with heat transfer.

## CONCLUSION

Entropy generation calculations were used to study the effect of an elliptic rotor's aspect ratio in a rotor-casing assembly at different angular speeds. Entropy generation results provide a better insight as to the local and global efficiency of a given rotor at different angular speeds. The results can be used to identify and quantify regions of high-energy losses. Overall, a rotor with an aspect ratio of 5 yields the best results in terms of low entropy generation.

## ACKNOWLEDGMENT

The authors would like to thank the Victorian Partnership for Advanced Computing (VPAC) for their support of this work under the Expertise Program Grant Scheme.

## REFERENCES

- ABU-HIJLEH, B. A/K (2000). "Modifying a Reattaching Shear Layer Using a Rotating Cylinder." *Journal of Computers and Fluids*, 29: 261-273.
- BEJAN A. (1982). *Entropy Generation Through Heat and Fluid Flow*, John Wiley & Sons, New York.
- Fluent Inc. (2002) FLUENT 6.0 manual. FLUENT, Lebanon, New Hampshire, 2003.
- HEISLER, H. (2001). *Vehicle and Engine Technology 2<sup>nd</sup> edition*, SAE publications, Warrendale.
- MOHAMMADI B. and PIRONNEAN O. (1993). *Analysis of the K-Epsilon Turbulence Model*, John Wiley & Sons, Chichester.
- TAKEI, N. and TAKABE, S. (1997), "Optimization in Performance of Lysholm compressor." *JSAE Review*, **18**, 331-338.

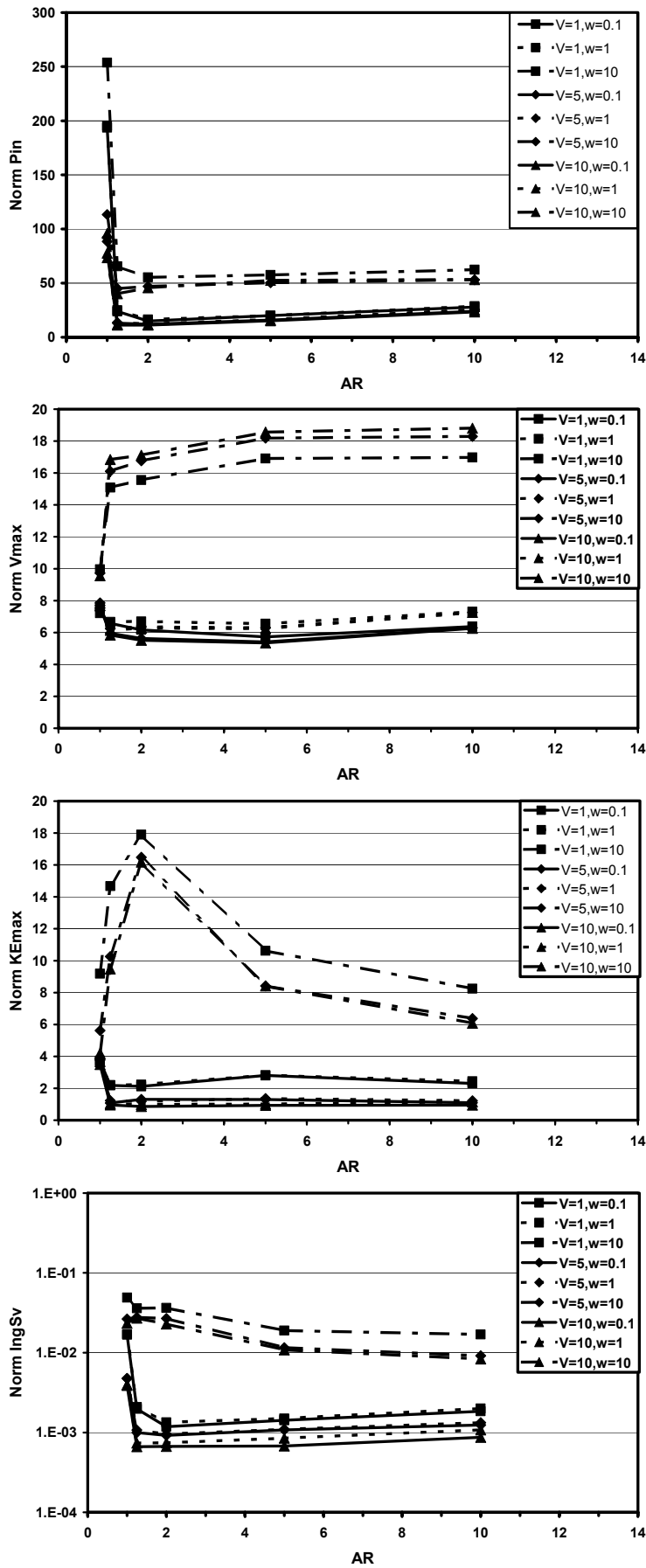


**Figure 3:** Changes in the normalized inlet pressure ( $P_{in}$ ), maximum velocity ( $V_{max}$ ), maximum kinetic energy ( $KE_{max}$ ), and total entropy generation ( $S_{tot}$ ) as a function of the rotor aspect ratio (AR) for the case  $CL=2\%$

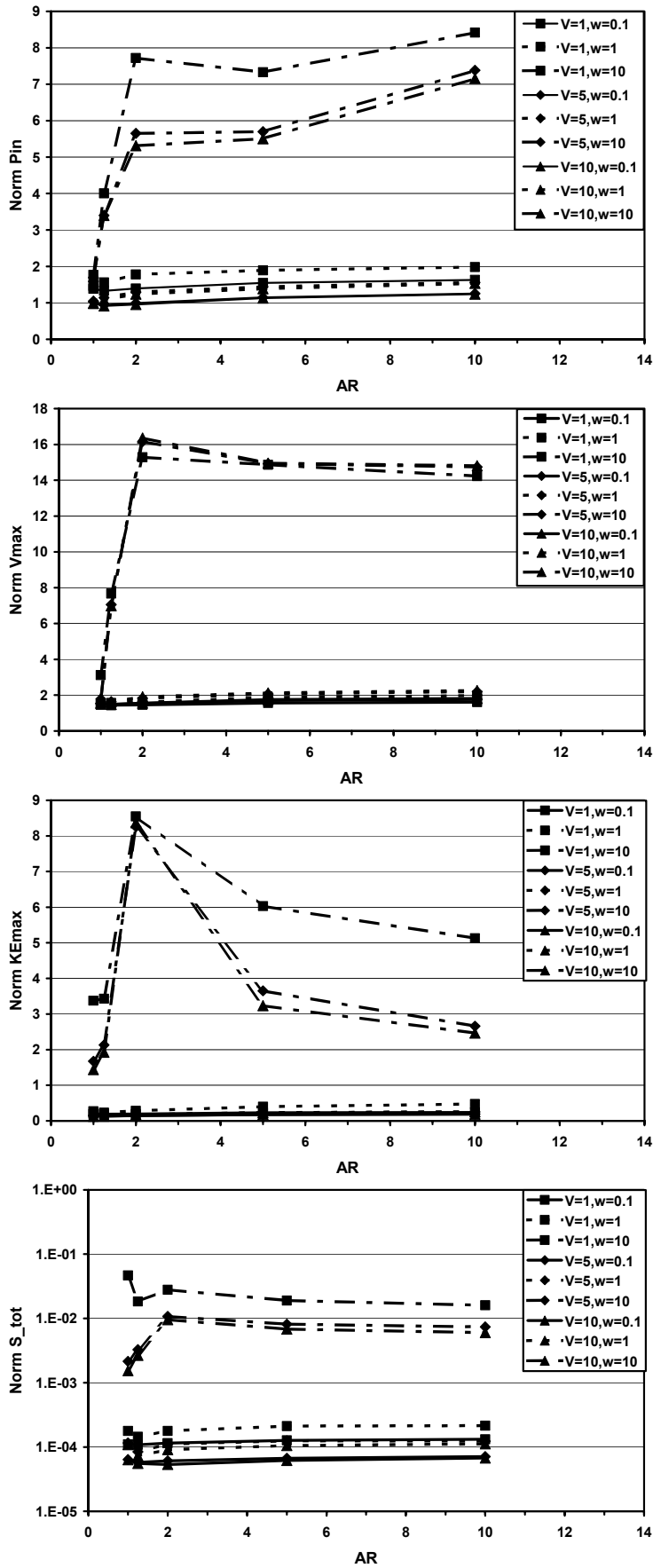


**Figure 4:** Changes in the normalized inlet pressure ( $P_{in}$ ), maximum velocity ( $V_{max}$ ), maximum kinetic energy ( $KE_{max}$ ), and total entropy generation ( $S_{tot}$ ) as a function of the rotor aspect ratio (AR) for the case  $CL=20\%$

